

Reflectometry measurements of the $m=1$ satellite mode
in L- and H-mode plasmas in ASDEX

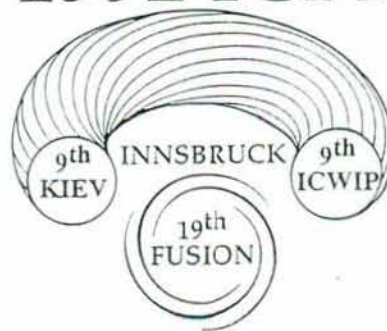
F. Serra, M. E. Manso, A. Silva, J. Matias, F. Wagner¹, H. Zohm¹, A. Kallenbach¹
and P. Varela

Centro de Fusão Nuclear, EURATOM/IST Association, 1096 Lisboa Codex, Portugal

¹Max-Planck Institut für Plasmaphysik, EURATOM/IPP Association, Garching

19th EPS Conference on Controlled Fusion and
Plasma Physics

1992 ICPP



INNSBRUCK, AUSTRIA, 29 JUNE - 3 JULY 1992

1 - Introduction

In ASDEX, with strong NBI heating, often a large central $m=1, n=1$ mode is observed on the SXR emission. For $P_{NBI} \geq 1$ MW a mode rotating with the same frequency, the so-called 'm=1 satellite', is seen on the magnetic pick-up coils in the L and H-phases. Magnetic measurements in the divertor chamber suggest that the satellite mode might be located outside the separatrix, on open field lines reaching the divertor /1/. Here we present results from localized microwave reflectometric measurements. The time evolution of the satellite mode frequency is studied for plasmas with different q_a and the mode localization is estimated, confirming that it should be close to but outside the separatrix. The central toroidal rotation velocities of the plasma can be inferred from the measured frequencies of the satellite modes.

2 - Local frequency spectra of the satellite mode

A set of H-mode deuterium discharges was analysed, with q_a at the edge between 2.6 and 3.8, where NBI (Deuterium co-injection, $P_{NI} \geq 2.3$ MW) was applied at $t = 1.2$ s after the start of the discharge. Two density layers were probed simultaneously with fixed frequency reflectometry at the plasma edge, in the range $(0.5 - 1.2) \times 10^{13} \text{cm}^{-3}$, and local power spectra of density fluctuations were obtained.

The frequency distribution of the fluctuations detected during two such discharges (# 32225, and # 32273) are shown, as contour plots, in Figs. 1 (a) and 2(a). The H_α traces (Figs.1(b) and 2(b)) are also presented.

In the example of Fig.1(a) (with $n_e = 0.5 \times 10^{13} \text{cm}^{-3}$), a $m=1$ satellite mode is detected, with frequency increasing from ~ 14 kHz in the L-phase to 24 kHz in the H-phase; identical frequencies are observed by Mirnov coils (Fig. 1(c)). The $m=1$ activity and the coupled mode disappear at the onset of the first sawtooth observed in the H phase and are destabilized again shortly before the second sawtooth. The frequencies then decrease as a corollary to the decrease of the toroidal plasma rotation; these modes are suppressed after the second sawtooth.

In the example of Fig. 2(a) (with $n_e = 0.6 \times 10^{13} \text{cm}^{-3}$) a short (ELM-free) H-mode is observed where the fluctuations are suppressed. At the second L-H transition, fluctuations again drop drastically and a coherent (satellite) mode coupled with central $m=1, n=1$ is clearly detected. Its frequency increases from $f_{L-H} \sim 18$ kHz at the end of the L-phase to a maximum $f_m \sim 24$ kHz just before the occurrence of the single ELM.

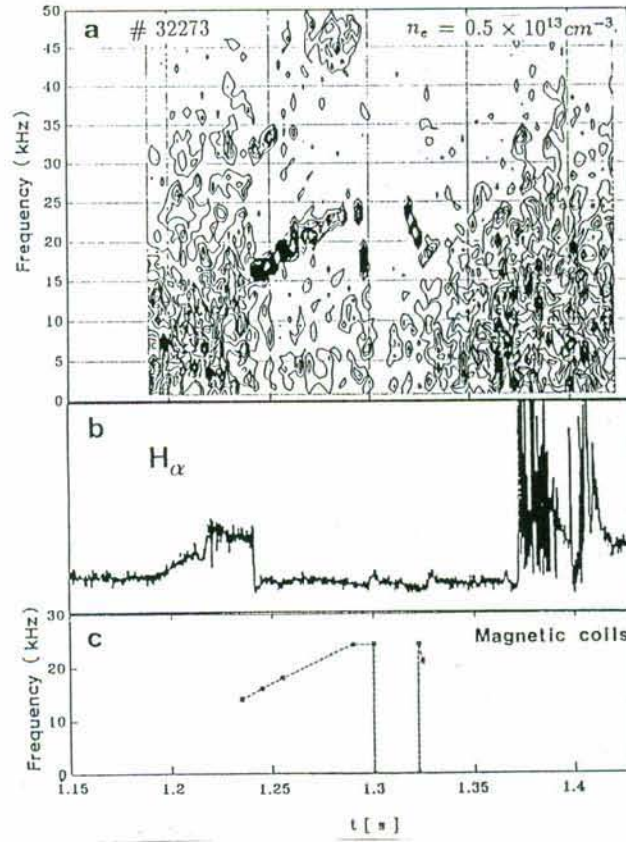


Fig. 1 (a) Contour plot of the power spectrum of density fluctuations, for # 32273, at $n_e = 0.5 \times 10^{13} \text{cm}^{-3}$; (b) H_α at the divertor; (c) frequency of the satellite mode obtained from magnetic measurements.

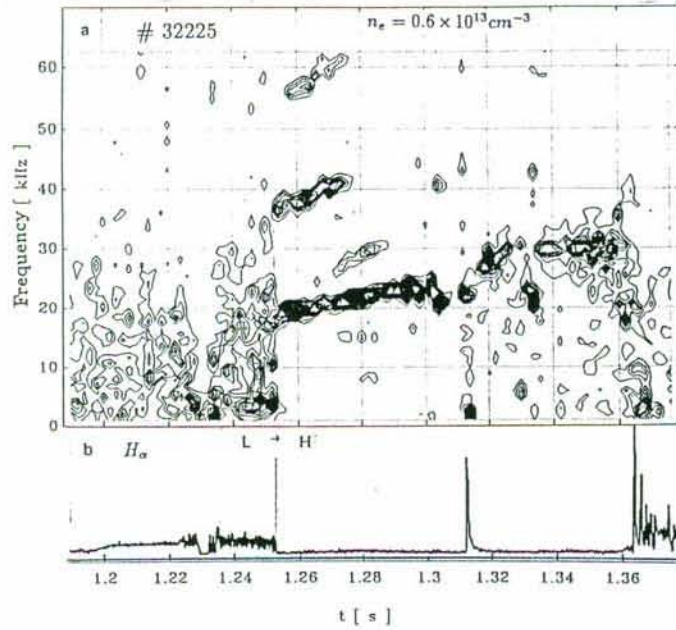


Fig. 2 (a) Contour plot of the power spectrum, for # 32225, at $n_e = 0.6 \times 10^{13} \text{cm}^{-3}$; (b) H_α at the divertor.

The frequencies of the satellite mode measured by reflectometry agree with Mirnov coil measurements that detect the mode during the L and H-phase, although with lower amplitude in the L-phase. As the layers probed by reflectometry in the L-phase are well inside the separatrix but the mode location is outside (as it will be discussed later) the mode is hardly seen by reflectometry before the L-H transition; the high level of turbulence makes it difficult to detect a coherent structure of low amplitude.

As shown in Fig. 3(a), the frequencies of the satellite mode grow during the H-phase, from f_{L-H} up to maximum observed values f_m . The highest value of the frequency represents a stationary level of the toroidal rotation velocity of the plasma. In some cases, before the saturation is reached, the (1,1) mode may be suppressed due to sawtooth events. In these cases the maximum observed value is below the saturated value. The minimum temporal rate of change of the frequency is observed at plasmas with $q_a \sim 3.3$ and the maximum for $q_a \sim 3.8$; in the example of # 32230 ($q_a = 3.8$) a late transition occurs (~ 80 ms after NBI) and the maximum observed frequency (30 kHz) is reached soon after (~ 10 ms), when the mode is suppressed.

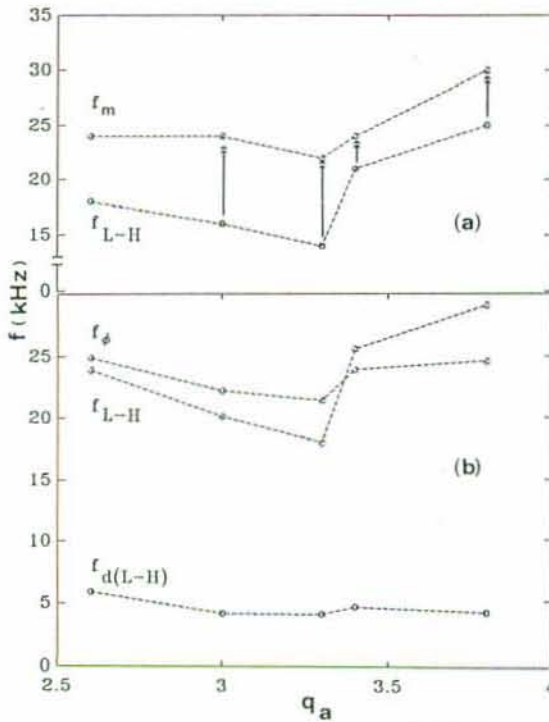


Fig.3 (a) Frequencies of the satellite mode at the transition, f_{L-H} , and maximum values (f_m) measured by reflectometry during the H-phase; (b) Comparison between f_ϕ and $f_{L-H} + f_d$ for different q_a plasmas.

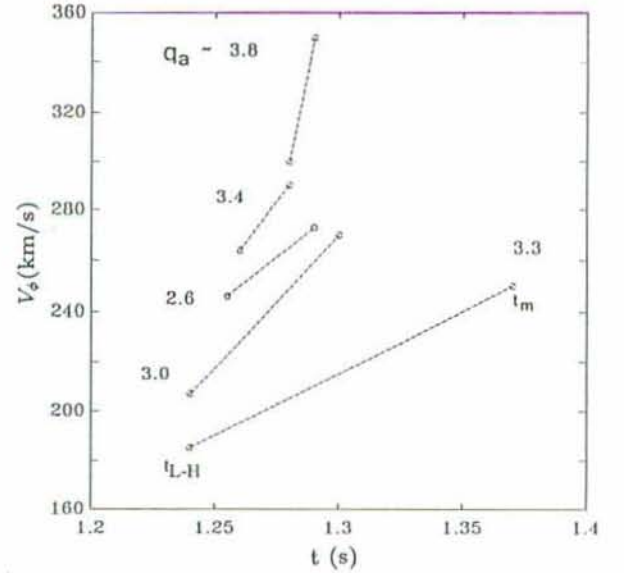


Fig.4 Estimate of the central toroidal rotation V_ϕ showing its increase from the transition (t_{L-H}) to a maximum in the H-phase (t_m).

3 - Relation of satellite frequency and plasma central toroidal rotation

As the magnetic field perturbation \dot{B} is expected to be frozen into the plasma, the measured frequency (f) of the satellite mode can give an estimate of the central toroidal rotation (f_ϕ) of the plasma. The existence of a pressure gradient in the plasma contributes locally with the diamagnetic electron drift frequency, which can be expressed as a purely toroidal contribution (f_d) to the mode frequency /1/. The central toroidal rotation velocity of the plasma can thus be roughly given (for co-injection) by $v_\phi = 2\pi R(f + f_d)$, where R is the plasma major radius and f_d is evaluated at the $q=1$ surface. In all the cases analysed there is a decrease in the drift frequency between t_{L-H} and t_m (due to the flattening of the profile close to the resonance surface), but a net increase of the toroidal rotation velocity is observed with maximum values in the range $\sim 250 - 350$ km/s (see Fig.4).

The obtained values of the toroidal rotation frequency at the L-II transition were compared with the frequency derived from the statistical analysis of charge exchange recombination (CXR) spectroscopy data, for co-injection L-mode discharges /2/:

$$f_\phi[kHz] = 30 \left(\frac{M}{\bar{n}_e} \right)^{0.61} \times I_p^{0.3}, \quad [MW, amu, 10^{19}m^{-3}, MA], \quad (1)$$

where $M \sim 1.2(A_b)^{1/2}P_{NI}[Nm]$ is the torque applied to the plasma, which is higher by deuterium beams ($A_b=2$) than by hydrogen ($A_b=1$). As (1) describes the central speed it slightly overestimates the velocity at the $q=1$ surface.

A good agreement is found between the values measured at the L-II transition and those predicted by the scaling law (1) (see Fig. 3(b)). The above comparison cannot be extended to the H-phase (where the total angular momentum of the plasma changes), as (1) only applies to stationary conditions.

In all the discharges analysed with deuterium an increase in the toroidal velocity during the H-phase is observed. This behaviour corresponds to early L-II transitions (~ 35 to 80 ms after beam injection), so the speeding up of the plasma may still last during the H phase. In contrast, in discharges with hydrogen injection the values measured for the satellite mode are constant and typically ~ 17 kHz. This is due to the fact that the transition L-H usually occurs later than in deuterium discharges (some 200 ms after the neutral beams start), so the rotation velocity of the plasma is already saturated at the beginning of the H-phase. These results confirm that for the same set of plasma parameters the speed attained with deuterium injection is higher than with hydrogen.

4 - Localization of the m=1 satellite mode

The effect of the coherent fluctuations induced by the satellite mode on the wave propagation can be described using the geometric optics approximation, as the scale length of the fluctuations is $l_c \geq \lambda_0$ (λ_0 : free space wavelength of the probing wave). Fluctuations (with frequency $\Omega \ll \omega_0$) cause mainly Doppler shifts of the phase φ due to the propagation in the plasma, $\varphi(t) = \varphi_c + \Delta\varphi \sin(\Omega t + \delta)$, leading to phase modulations of the detected reflectometric signals ($V(t)$):

$$V(t) \sim \frac{1}{2} + \frac{A^2 J_0(\Delta\varphi)}{2} + A J_0(\Delta\varphi) \cos\varphi + \sum_{n=1}^{\infty} 2A J_{2n}(\Delta\varphi) \cos 2n\Omega t \cos\varphi - \sum_{n=0}^{\infty} 2A J_{2n+1}(\Delta\varphi) \sin(2n+1)\Omega t \sin\varphi + \dots (2)$$

where $J_n(\Delta\varphi)$ is the Bessel function of the first kind, and of order n . The phase modulation $\Delta\varphi$ can be obtained from the relative amplitude of the harmonics (odd or even) of the frequency (Ω) /3/.

A relation between the amplitude of the fluctuating phase change and the amplitude of the density fluctuation causing it depends on the scale length of the perturbation and its radial location along the wave propagating path. An accurate measurement of the amplitude of the the density fluctuations will therefore imply insight of the characteristics of the fluctuations, as well as the consideration of 2D-geometry effects; this has been stressed in recent studies using the full wave (1D) solution /4/.

Assuming perturbations centered at the reflecting layer (x_c), causing local modulations of the density profile, a simple relation between the amplitude of the fluctuations, ($\delta n_e/n_e$) at x_c , and $\Delta\varphi$ is obtained (for a profile with density gradient ∇n):

$$\frac{\delta n_e}{n_e} = \frac{3\lambda_0}{8\pi} \left(\frac{\nabla n}{n} \right)_{x_c} \Delta\varphi \quad (3)$$

A comparison of the estimated values of $\delta n_e/n_e$ at two different layers was done using two reflectometry channels (with frequencies f_I and f_{II}) operating along the same line of sight. Fig. 5 shows the frequency spectra of fluctuations, (# 32225), at the plasma layers: (I) $n_e = 0.6 \times 10^{13} \text{ cm}^{-3}$ ($f_I = 22 \text{ GHz}$), and (II) $n_e = 0.98 \times 10^{13} \text{ cm}^{-3}$ ($f_{II} = 28 \text{ GHz}$), for four time intervals from (1) immediately after the L-H transition to (4) ~ 15 ms after L-H.

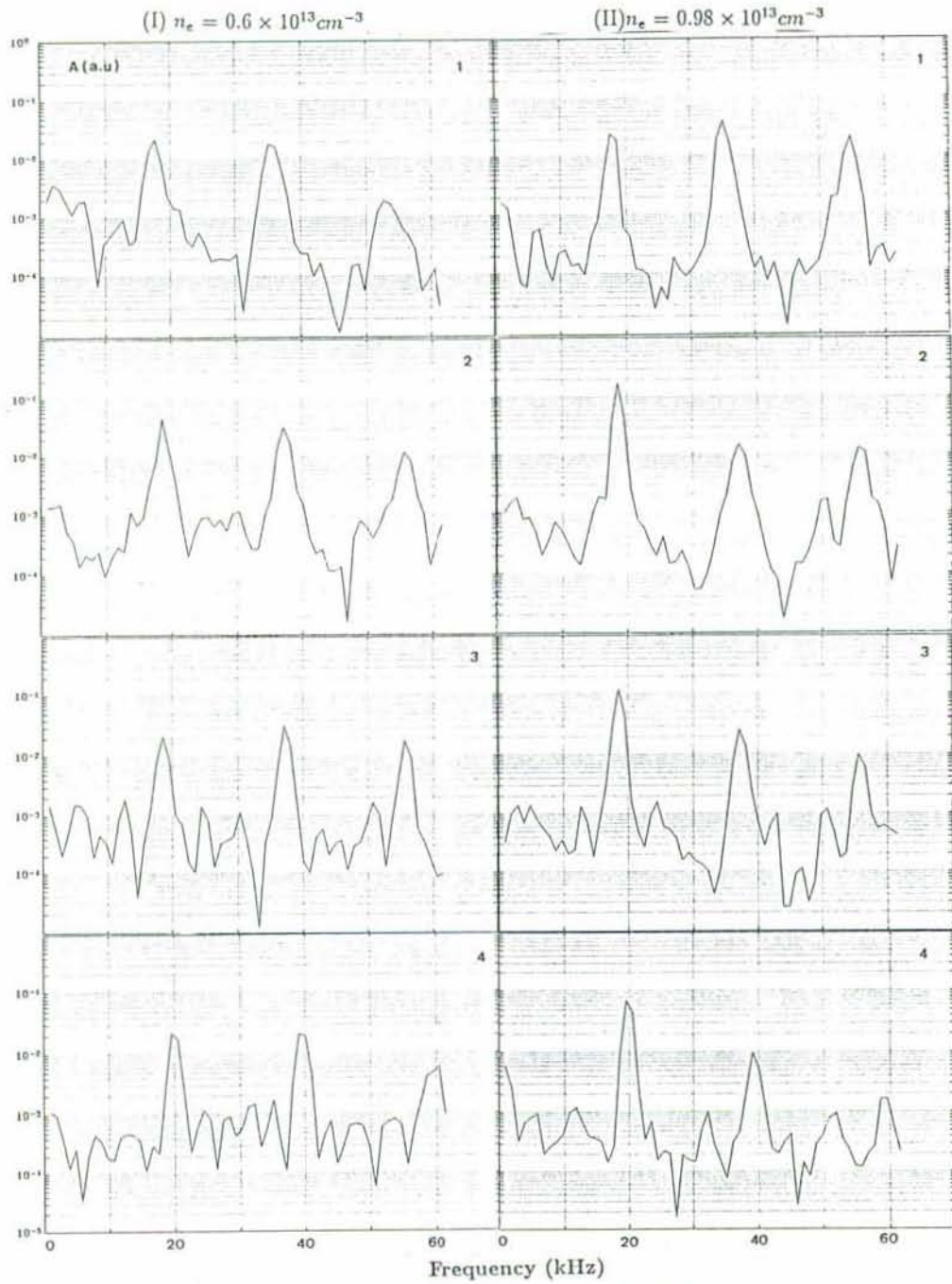


Fig. 5 Power spectrum of density fluctuations (# 32225) for (1): $\Delta t = 1254-56$ ms; (2): 1262-64 ms; (3): 1264-66 ms; (4): 1268-70 ms.

Three harmonics are observed in the spectra due to the modulating frequency of the perturbation ($\Omega/2\pi$ increases from ~ 18 kHz in a) to ~ 20 kHz in d)). From the ratio between the first and third harmonic, $J_1(\Delta\varphi)/J_3(\Delta\varphi)$, the values of the amplitude $\Delta\varphi$ were estimated. For high values of $\Delta\varphi$ the second harmonic J_2 may exceed J_1 (for $\Delta\varphi \geq 2.7$); in the cases where $\Delta\varphi$ approaches 3.0 the amplitude of J_3 is close to J_1 (see Table 1).

(I) $n_e = 0.6 \times 10^{13} \text{cm}^{-3}$ (II) $n_e = 0.98 \times 10^{13} \text{cm}^{-3}$

Δt	J_1/J_3	$\Delta\varphi$	$\delta n/n(\%)$	J_1/J_3	$\Delta\varphi$	$\delta n/n(\%)$
(1)	12.11	1.32	10.8	1.18	2.95	11.5
(2)	3.93	2.09	22.7	13.21	1.28	6.7
(3)	1.24	2.92	31.8	12.22	1.32	6.9
(4)	3.51	2.18	26.6	42.83	0.74	4.3

Table 1

The temporal evolution of the plasma density profile was modelled from O-mode broadband reflectometry for similar discharges /5/. Data obtained from #32031 was used (see Fig.6); during the L-phase, with low density gradient ($\sim 0.15 \times 10^{13} \text{cm}^{-4}$), the probed layers would be accordingly located at $r \leq 40 \text{cm}$, inside the magnetic separatrix.

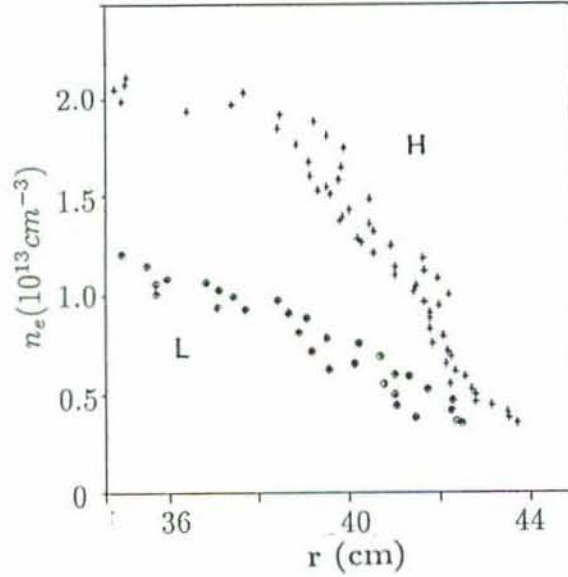


Fig.6 Density profiles from broadband reflectometry (# 32031) for the L- phase, and for the H-phase $\sim 10 \text{ms}$ after the L-H transition.

Immediately after the transition the gradient at the edge increases to $\sim 0.3 \times 10^{13} \text{cm}^{-4}$ and reaches $\sim 0.4 \times 10^{13} \text{cm}^{-4}$ at $\sim 10 \text{ms}$ after L-H; by that time the position of the layers probed at fixed density is estimated to be at (I) $r \sim 43 \text{cm}$ and (II) $r \sim 42 \text{cm}$. From eq. (3) it can be concluded that at the inner layer, (II), the rate of fluctuations decreases from $\sim 11.5\%$ near t_{L-H} to $\sim 6.9\%$ after $\sim 10 \text{ms}$ (see Table 1); during the same time interval, the rate of fluctuations at the outer layer, (I), increases from $\sim 10.8\%$ to a maximum $\sim 31.8\%$. The localization of the mode should therefore have shifted outwards from a region around 42cm , to $r \geq 43 \text{cm}$. This is consistent with a mode location close to and outside the magnetic separatrix and a movement outwards during the H-phase by $\geq 1 \text{cm}$.

The spectral analysis shows a subsequent decrease in the rate of fluctuations at both layers. As the probed layers are now roughly at fixed radial positions (the build up of the density gradient at the edge is completed $\sim 20 \text{ms}$ after L-II), the decrease of the fluctuations suggests therefore that the mode is being displaced further outwards following the displacement of the magnetic separatrix.

5 - Conclusions

The temporal evolution of the so-called "m=1 satellite mode" (coupled to the central m=1,n=1 activity) is studied with microwave reflectometry in H-mode plasmas with q_a between 2.6 and 3.8.

The central toroidal velocities of the plasma are inferred from the measured mode frequencies, which increase during the H-phase for the deuterium co-injection discharges; a maximum temporal rate of change of the velocity is obtained for plasmas with $q_a \sim 3.8$, and a minimum for $q_a \sim 3.3$.

The localization of the mode is obtained from density profile reflectometry measurements and from the analysis of the local frequency spectra. Results show that the mode should be localized close to and outside the magnetic separatrix, giving further evidence to the previous estimates based on magnetic measurements /1/. During the H-phase the maximum amplitude of the mode is observed to shift outward by ≥ 1 cm, suggesting that the mode is radially moving outward together with the magnetic separatrix.

References

- /1/ O. Klüber et al., Nuclear Fusion, Vol. 31, No. 5, 907 (1991).
- /2/ A. Kallenbach et al., Nuclear Fusion, Vol. 30, No. 4, 645 (1990).
- /3/ E. Mazzucato, Report MATT 1151, Plasma Phys. Lab., Princeton (1975).
- /4/ J. Garcia, M. Manso, J. Mendonca and F. Serra, Proc. 16th Europ. Conf. on Contr. Fusion and Plasma Physics, Vol. IV, 1251 (1989); X.L. Zou, L. Laurent and J. Rax, Report EUR-CEA-FC 1412, Cadarache (1990); N. Bretz, Report PPPL-2795 Princeton Univ. (1991); P. Cripwell, PhD Thesis, JET (1992).
- /5/ M. E. Manso et al., 18th Eur. Conf. Berlin, Vol. 15C, I-393 (1991).